Cholesterol-dependent retention of GPI-anchored proteins in endosomes

Satyajit Mayor[1], Shefali Sabharanjak and Frederick R.Maxfield[2]

National Centre for Biological Sciences, TIFR Centre, Bangalore 560012, India and [2]Department of Biochemistry, Cornell University Medical College, New York, NY 10021, USA

[1]Corresponding author
e-mail: mayor@ncbs.tifrbng.res.in

Several cell surface eukaryotic proteins have a glycosyl-phosphatidylinositol (GPI) modification at the C-terminal end that serves as their sole means of membrane anchoring. Using fluorescently labeled ligands and digital fluorescence microscopy, we show that contrary to the potocytosis model, GPI-anchored proteins are internalized into endosomes that contain markers for both receptor-mediated uptake (e.g. transferrin) and fluid phase endocytosis (e.g. dextrans). This was confirmed by immunogold electron microscopy and the observation that a fluorescent folate derivative bound to the GPI-anchored folate receptor is internalized into the same compartment as co-internalized horseradish peroxidase–transferrin; the folate fluorescence was quenched when cells subsequently were incubated with diaminobenzidine and H_2O_2. Most of the GPI-anchored proteins are recycled back to the plasma membrane but at a rate that is at least 3-fold slower than C_6-NBD-sphingomyelin or recycling receptors. This endocytic retention is regulated by the level of cholesterol in cell membranes; GPI-anchored proteins are recycled back to the cell surface at the same rate as recycling transferrin receptors and C_6-NBD-sphingomyelin in cholesterol-depleted cells. Cholesterol-dependent endocytic sorting of GPI-anchored proteins is consistent with the involvement of specialized lipid domains or 'rafts' in endocytic sorting. These results provide an alternative explanation for GPI-requiring functions of some GPI-anchored proteins.
Keywords: cholesterol/endocytosis/folate receptor/GPI anchoring/retention

Introduction

A diverse set of cell surface eukaryotic proteins including several receptors, enzymes and adhesion molecules have a glycosylphosphatidylinositol (GPI) moiety at their C-terminal end that serves as a membrane anchor (Field and Menon, 1992; McConville and Ferguson, 1993). This ubiquitous protein modification has been implicated in a variety of cell biological processes (Ferguson, 1994). It acts as an apical targeting signal for proteins in some epithelial cell types via its association with putative glycolipid rafts in the *trans*-Golgi network (TGN) (Harder and Simons, 1997). GPI anchoring has also been shown to be important for the intracellular signaling capacity of several proteins especially in lymphocytes (Robinson, 1991; Brown, 1993).

Although in immunolocalization studies GPI-anchored proteins were reported to be clustered at the cell surface, with a significant fraction of the clusters associated with 50–60 nm caveolin/VIP-21-coated membrane invaginations called caveolae (Rothberg *et al.*, 1992; Dupree *et al.*, 1993), we and others have shown that these proteins are not constitutively concentrated in caveolae (Mayor *et al.*, 1994; Parton *et al.*, 1994; Mayor and Maxfield, 1995; Fujimoto, 1996). Instead, they are enriched in these structures only after cross-linking with polyclonal secondary antibodies.

Numerous GPI-anchored proteins are internalized and recycled back to the cell surface (Kamen *et al.*, 1988; Lisanti *et al.*, 1990; Rothberg *et al.*, 1990b; Taraboulos *et al.*, 1990; Keller *et al.*, 1991; Borchelt *et al.*, 1992). It was proposed that GPI-anchored proteins are internalized via the pinching off of caveolae in a process called potocytosis (Keller *et al.*, 1991; Anderson, 1993; Turek *et al.*, 1993). The findings that these proteins are distributed diffusely at the cell surface, being neither enriched nor excluded from coated and non-coated pits at the cell surface, reopened the question about the mechanisms and pathways involved in the internalization and trafficking of GPI-anchored proteins. Electron microscopic studies have shown that GPI-anchored folate receptors are in endosomes (Birn *et al.*, 1993; Rijnboutt *et al.*, 1996). However, a recent study used cell fractionation to study the uptake of 5-methyltetrahydrofolate via GPI-anchored folate receptors and reported that the folate was not found in endosomes in MA104 cells, suggesting that folate was transported to the cytoplasm without passage through endosomes (Smart *et al.*, 1996). Thus, there are conflicting interpretations of the endocytic itinerary followed by GPI-anchored proteins and their ligands.

Regardless of the initial step in internalization, the endocytic trafficking of GPI-anchored proteins has features that are different from that of other membrane components. For example, the recycling of folate receptors in MA104 cells (Kamen *et al.*, 1988) is significantly slower than the typical recycling rates of lipids or recycling receptors (Koval and Pagano, 1989; Mayor *et al.*, 1993). This could be consistent either with a specialized endocytic pathway (Anderson, 1993) or with altered kinetics of passage through the typical endocytic recycling itinerary.

To study the intracellular trafficking pathways of GPI-anchored proteins, we have used the GPI-anchored folate receptor as a model since its kinetics of trafficking have been studied extensively (Kamen *et al.*, 1988, 1989; Hjelle

et al., 1991; Birn *et al.*, 1993). We have employed quantitative fluorescence microscopy of a fluorescent analog of folic acid [N^{α}-pteroyl-N^{ε}-(4′-fluorescein-thiocarbamoyl)-L-lysine (PLF)] which binds the folate receptor monovalently and with an affinity similar to folic acid (McAlinden *et al.*, 1991; Mayor and Maxfield, 1995). Here we show that GPI-anchored proteins are endocytosed into sorting endosomes that contain markers for both receptor-mediated uptake and fluid phase endocytosis. The GPI-anchored proteins then follow the endocytic recycling route but at a rate that is 3-fold slower than N-[N-(7-nitro-2,1,3-benzoxadiazol-4-yl)-ε-aminohexanoyl]-sphingosyl-phosphorylcholine (C_6-NBD-SM) or recycling transferrin receptors. We find that the GPI-anchored proteins are retained mainly in the peri-centriolar endocytic recycling compartment in Chinese hamster ovary (CHO) fibroblasts. Here we show for the first time that sorting/retention in the endocytic pathway is dependent on lipid levels in cell membranes since in cholesterol-depleted cells GPI-anchored proteins are no longer retained relative to C_6-NBD-SM or other recycling transmembrane proteins such as the transferrin receptor.

Results

Uptake of a fluorescent folate analog in MA104 cells

To validate the use of PLF as a reagent to study the trafficking of the GPI-anchored folate receptor, MA104 cells were incubated with PLF at 37°C for 0–3 h, and the fluorescence intensity was measured. The binding of PLF is competed effectively by unlabeled folic acid (1 μM; data not shown). Figure 1A shows the time-dependent increase in cell-associated PLF, relative to the surface binding (1 h at 0°C). When steady-state labeling has been achieved at 37°C, twice as much PLF binds to these cells compared with binding at 0°C. This indicates that unoccupied internal receptors are delivered to the surface and become available for binding PLF. As described in Materials and methods, the kinetics of approach to steady state reflect the rate of export of the folate receptor to the cell surface with a rate constant of 0.023/min ($t_{1/2}$ ~30 min) if we assume a single first order kinetic process. It is possible that there is more than one process for delivery of folate receptors to the surface, but the data fit within experimental error as a single first order process (Figure 1A). The kinetics of PLF association with MA104 cells are similar to the results reported for [^{3}H]folic acid (Kamen *et al.*, 1988).

Figure 2A shows the distribution of PLF fluorescence after binding to MA104 cells at 0°C. This fluorescence is consistent with uniform surface labeling containing some brightness variations due to membrane topography. After 37°C incubation (Figure 2B), there is an accumulation of fluorescence near the center of the cell. The diffuse surface fluorescence could be removed by incubation of the cells at 0°C with acid saline, while the perinuclear fluorescence in Figure 2B is not acid-releasable, confirming that it is internalized (data not shown).

Trafficking of GPI-anchored proteins in CHO cells

We characterized the trafficking pathway of endocytosed folate receptors in a CHO cell line which expresses a transfected human transferrin receptor and human GPI-anchored folate receptor (FRαTb-1 cells; Mayor and Maxfield, 1995). The distribution of PLF fluorescence after binding to FRαTb-1 cells at 0°C is also consistent with uniform surface labeling (Figure 2C). After 37°C incubation, there is an accumulation of fluorescence near the center of the cell (Figure 2D).

To measure the relative size of the surface and internal pools of receptors in FRαTb-1 cells, cell-associated PLF was measured at 0°C (Figure 1B, Surface) or after 3 h at 37°C (Figure 1B, Total). As with endogenous folate receptors in MA104 cells, at steady state about half the transfected folate receptors in FRαTb-1 cells are on the surface. When surface receptors were blocked by pre-incubation with folate at 0°C, and the cells were then incubated with PLF for 3 h at 37°C, internal receptors came to the surface and became labeled (Figure 1B, Internal). The time dependence of delivery of unoccupied receptors to the cell surface is shown in Figure 1C. In this experiment, the surface receptors had been blocked by pre-incubation with unlabeled folate at 0°C, so only newly externalized receptors would bind the PLF. The export of receptors to the cell surface is well described as a single first order process with a rate constant of 0.022/min (Figure 1C).

To rule out the possibility that the delivery of unoccupied folate receptors to the surface had a large component of biosynthetic delivery of folate receptors, we repeated the experiment shown in Figure 1C in the presence of cycloheximide. The data obtained in the presence of cycloheximide are similar to those obtained in its absence (compare open circles with closed circles in Figure 1C), confirming that the kinetics of approach to steady state are measuring mainly the export of recycling folate receptors.

To characterize the kinetics of endocytosis and the trafficking pathway of a different GPI-anchored protein in CHO cells, we measured the trafficking of decay accelerating factor (DAF) in a DAF-expressing CHO cells which also expresses the human transferrin receptor (DAFTb-1; Mayor and Maxfield, 1995) using labeled Fab fragments of an anti-DAF mouse monoclonal antibody (mAb). The time course of labeling DAFTb-1 cells with the Cy3-labeled Fab fragment of anti-DAF monoclonal antibody (Cy3-anti-DAF) at 37°C is shown in Figure 1D. The $t = 0$ time point in Figure 1D is the cell-associated Cy3-anti-DAF after a 3 h incubation at 0°C. For all other time points, the cells were incubated with Cy3-anti-DAF for the indicated time at 37°C. The export of unlabeled DAF to the surface is well described as a single first order process ($k_e = 0.028$/min; Figure 1D), although again we cannot rule out undetected contributions from additional processes.

The externalization rate constants for folate receptor and DAF are similar, and both are ~3-fold lower than the rate constants for externalization of recycling transferrin receptors in TRVb-1 cells (Table I).

Endocytic route of GPI-anchored proteins in CHO cells

The pathways of several different endocytosed molecules have been characterized in the parent CHO cell line TRVb-1 cells (from which DAFTb-1 and FRαTb-1 have been derived; McGraw *et al.*, 1991). Recycling receptors,

membrane markers and lysosomally directed molecules are first detected in peripheral compartments called sorting endosomes. Recycling molecules are removed from these endosomes with a $t_{1/2}$ of 2–3 min, and then they are delivered to a peri-centriolar compartment called the endocytic recycling compartment (Dunn *et al.*, 1989; Mayor *et al.*, 1993; Mukherjee *et al.*, 1997). Lysosomally directed molecules continue to accumulate in the vacuolar portion of the sorting endosomes which form late endosomes with a $t_{1/2}$ of ~8 min (Salzman and Maxfield, 1988; Dunn and Maxfield, 1992).

To observe the endocytic compartments that folate receptors traverse, we incubated FRαTb-1 cells at 37°C

with PLF and Cy3-labeled transferrin (Cy3-Tf) for 3 h. Surface-bound Cy3-Tf and PLF were removed by acid stripping. Both PLF (Figure 3A) and Cy3-Tf (Figure 3B) were found in peripheral endosomes (arrows) and central compartments (arrowheads). A major site for intracellular accumulation of the PLF-labeled folate receptor overlaps the fluorescence of Cy3-Tf in the endocytic recycling compartment near the cell center. Many of the peripheral compartments also contain both probes. However, the relative intensities of the two probes were different in the two compartments; the folate receptor is distributed somewhat more peripherally than the transferrin receptors. These data indicate that at steady state there is considerable
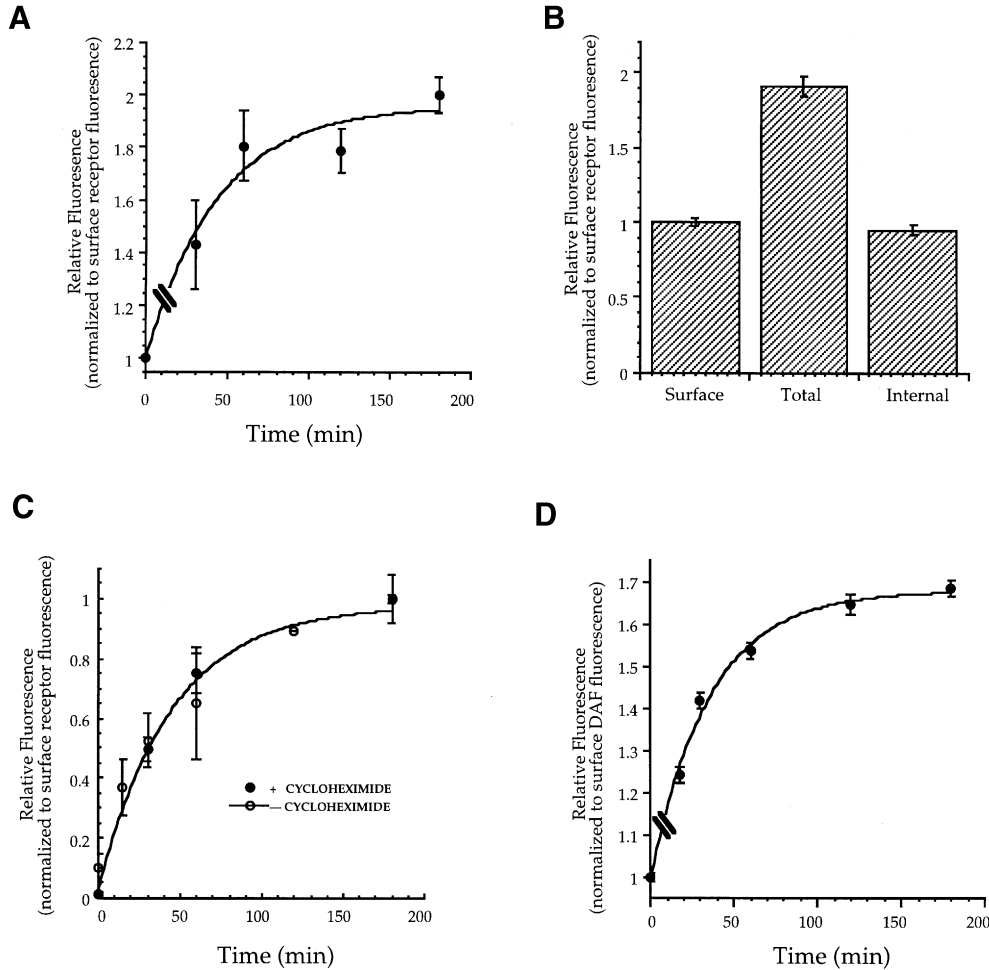
Fig. 1. Trafficking kinetics of GPI-anchored proteins in MA104 cells and CHO cells. (**A**) MA104 cells were incubated with 10 nM PLF for 1 h at 0°C (Surface binding; $t = 0$) or for 30 min to 3 h at 37°C and then taken for analysis of PLF binding by quantitative fluorescence microscopy. Each data point is an average of two independent experiments. Data for each experimental condition were obtained from two separate dishes from which 9–10 fields per dish were imaged. The points were fitted to a curve $y = 1 + 0.97 \times [1 - e^{(-0.023t)}]$ by the method of least squares ($R > 0.97$). Error bars in all panels represent standard errors. (**B**) FRαTb-1 cells were incubated with 10 nM PLF for 3 h at 0°C (Surface) or 37°C (Total). Internal receptors (Internal) were determined by first incubating the cells at 0°C with 30 nM folic acid, prior to labeling with 10 nM PLF at 37°C for 3 h. PLF binding was determined by quantitative fluorescence microscopy. Each data point is an average of four independent experiments. Data for each experimental condition were obtained from two separate dishes from which 9–10 fields per dish were imaged. Data from individual experiments were combined by normalizing to the 0°C (Surface) condition. (**C**) FRαTb-1 cells were incubated in the presence of cycloheximide (●; 25 μg/ml) or without cycloheximide (○) for 1 h prior to incubation with 30 nM folic acid for 1 h at 0°C to saturate cell surface folate receptors. After rinsing with folate-free F-12 medium, the cells were incubated further for the indicated times with 10 nm PLF at 37°C in the continuous presence (●) or absence of cycloheximide (○). Total PLF binding to internal receptors was quantified for each time point. The data shown are an average of three independent experiments. The points (○) were fitted to a curve $y = 0.025 + 0.95 \times [1 - e^{(-0.022t)}]$ by the method of least squares ($R > 0.98$). (**D**) DAFTb-1 cells were incubated with Cy3-anti-DAF Fab (25 μg/ml) for 3 h at 0°C (surface; $t = 0$) or for 20 min to 3 h at 37°C. At the end of the incubations, the cells were rinsed and taken for analysis of Cy3-anti-DAF binding by quantitative fluorescence microscopy. Each data point is an average of two independent experiments. Data for each experimental condition were obtained from two separate dishes from which 9–10 fields per dish were imaged. Data from individual experiments were combined by normalizing to the 0°C (surface) condition. The points were fitted to a curve $y = 1 + 0.7 \times [1 - e^{(-0.028t)}]$ by the method of least squares ($R > 0.99$).

overlap in the distribution of transferrin receptors and folate receptors, but there may be quantitative differences in their partitioning among the compartments. In a separate experiment, we found that the major site for the intracellularly retained DAF also overlaps the endocytic recycling compartment and the peripheral endosomes (data not shown).

To characterize better the early steps in the pathway taken by the folate receptor and DAF after internalization, we co-incubated cells with PLF and Cy3-Tf (Figure 3C and D) or Cy3-anti-DAF and fluorescein-labeled Tf (data not shown) for short periods. GPI-anchored proteins are internalized into endosomes that are co-localized extensively with Tf-containing endosomes. After a 10 min continuous incubation, a substantial fraction of transferrin has passed from the peripheral sorting endosomes into the peri-centriolar endocytic recycling compartment (Figure 3D). The GPI-anchored proteins have also started to move into the recycling compartment, but the relative distribution of the GPI-anchored proteins may be more heavily weighted to the peripheral endosomes than is the case for transferrin (Figure 3C). This would suggest a slower rate
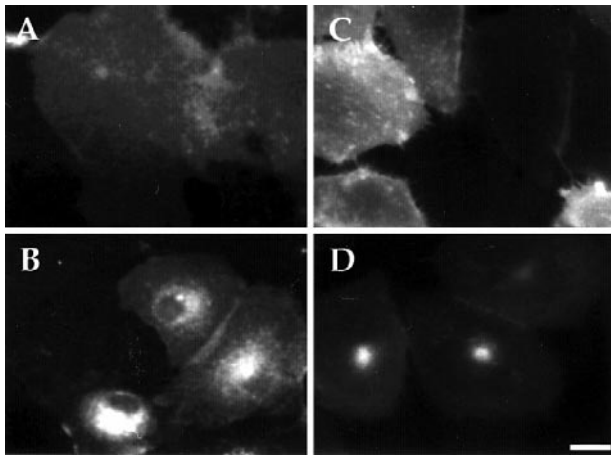
Fig. 2. Visualization of folate receptors in MA104 and CHO cells. MA104 cells (**A** and **B**) or FRαTb-1 cells (**C** and **D**) were incubated with 10 nM PLF for 3 h at 0°C (A and C) or 37°C (B and D) and then rinsed and taken for visualization of PLF fluorescence by digital fluorescence microscopy. Bar = 20 μm.

of exit of the GPI-anchored proteins from the peripheral sorting endosomes. However, this is a subtle effect that will require further investigation.

If the peripheral endosomes that contain GPI-anchored proteins are sorting endosomes, they should also accumulate fluid markers at short incubation times (Gruenberg and Maxfield, 1995; Mukherjee *et al.*, 1997). To confirm that the peripheral compartments are sorting endosomes, we co-internalized fluorescein-labeled dextrans with Cy3-anti-DAF (Figure 3E and F). After an 8 min incubation, we found that the two fluorophores are co-localized extensively. These observations show that GPI-anchored proteins are internalized into sorting endosomes and then leave the sorting endosomes and are delivered to the endocytic recycling compartment.

Although GPI-anchored proteins appeared to be in endosomes that also contain transferrin, it was possible that the two proteins were in separate compartments that were unresolvable using light microscopy. This was particularly a concern in the center of the cell where many organelles are concentrated. To determine if this was the case, we devised an assay that would indicate the presence of transferrin and PLF in the same intracellular compartment. This assay is based on the property of horseradish peroxidase (HRP) to generate reactive species when incubated with di-amino benzidine (DAB) and hydrogen peroxide (H_2O_2), which are capable of quenching fluorescence (Angelov *et al.*, 1995). Figure 4 shows that the formation of the HRP reaction products by HRP-labeled Tf (HRP-Tf) in endosomes resulted in almost complete loss of internal endocytic PLF fluorescence (Figure 4A) as compared with cells that had been incubated without HRP-Tf (not shown) or when HRP-Tf uptake was competed by unlabeled Tf (100-fold excess; Figure 4C). To rule out the possibility that the reactive species that are generated by the HRP reaction are able to cross intracellular membranes, we labeled cells at the surface with HRP-Tf (not shown), or filled late endosomes and lysosomes with free HRP using a 1 h pulse followed by a 3 h chase. Under these conditions, the HRP reaction with DAB did not result in any significant loss of PLF fluorescence (Figure 4B). Similarly, HRP-Tf did not quench a fluorescent

Table I. Effect of cholesterol depletion on the exocytic and internalization rates of GPI-anchored proteins

Cell line	Membrane markers	Treatment[a]	Internal = $\frac{L \cdot R_{i,ss}}{L \cdot R_s}$ Surface	Externalization rate (k_e/min)	Internalization rate (k_i/min)
MA104	folate receptor	–	1.0038 (0.09)	0.023 (0.001)	0.023 (0.09)
FRαTb-1	folate receptor	–	0.979 (0.063)	0.022 (0.004)	0.022 (0.004)
FRαTb-1	folate receptor	cholesterol depleted	0.41 (0.025)	0.075 (0.0154)	0.030 (0.007)
DAFTb-1	DAF	–	0.748 (0.034)	0.028 (0.003)	0.021 (0.002)
DAFTb-1	DAF	cholesterol depleted	0.348 (0.027)	0.061 (0.016)	0.021 (0.006)
FRαTb-1	NBD-SM	–	–	0.075 (0.006)	–
FRαTb-1	NBD-SM	cholesterol depleted	–	0.061 (0.004)	–
TRb-1[b]	TfR	–	–1.67 (0.005)	0.081 (0.02)	0.135 (0.025)
TRVbΔ3-59[b]	Δ3-59-TfR	–	0.412 (0.019)	0.08 (0.02)	0.033 (0.001)
TRVbΔ3-59[c]	Δ3-59-TfR	cholesterol depleted	0.285 (0.03)	0.068 (0.027)	0.019 (0.002)

The exocytic rate (k_e) and surface and internal pools were determined experimentally as described in Materials and methods. The internalization rate (k_i) and the internal to surface ratio were determined by rearrangements of Equation (5).
[a]Cholesterol depletion, where indicated, was carried out as described in the text.
[b]Data for these cell lines were obtained from Johnson *et al.* (1993).
[c]The exocytic rate constant and surface to internal ratios were determined from an approach to steady state experiment exactly as described in Johnson *et al.* (1993).
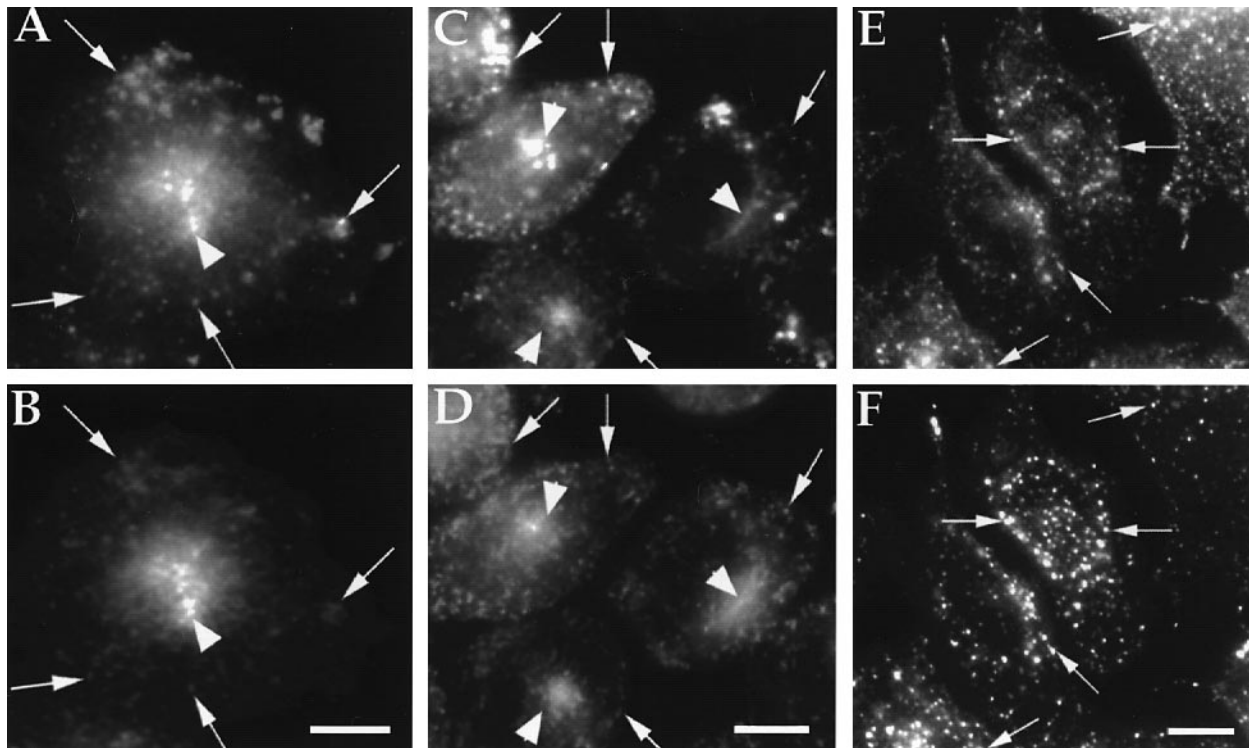
Fig. 3. Co-localization of GPI-anchored proteins with endocytic markers. FRαTb-1 cells were incubated with 10 nM PLF (**A** and **C**) and 5 µg/ml Cy3-Tf (**B** and **D**) for 3 h (A and B) or 10 min (C and D) at 37°C. The cells were rinsed in ice-cold medium 1 followed by ice-cold acid acid saline (pH 3.5), and neutralized with medium 1. Alternatively, DAFTb-1 cells were incubated with Cy3-anti-DAF (**E**) and 1 mg/ml F-dextran (**F**) for 8 min at 37°C and processed for microscopy. The cells were then taken for visualization of fluorescein fluorescence (A, C and F) and Cy3 fluorescence (B, D and E) by digital fluorescence microscopy. Arrows indicate peripheral endosomes and arrowheads indicate central fluorescence which is presumably recycling compartments. Bar = 10 µm.

antibody delivered to the TGN via a TGN38 construct (F.R.Maxfield, unpublished).

Quantitative analyses of PLF fluorescence after different treatments with HRP-Tf are shown in Figure 4D. HRP-Tf-generated DAB reaction products quenched 68 ± 7% ($n = 6$) of internal PLF fluorescence, and competition with excess unlabeled transferrin restored PLF fluorescence to untreated levels. PLF fluorescence was relatively unaffected by the DAB/H_2O_2 reaction if HRP-Tf was pulsed into cells for 40 min along with PLF and then chased out of the cells during the remaining 140 min of the incubation (Figure 4D, Chase Out). Free HRP added at the same concentration as HRP-Tf quenched a negligible fraction of internal PLF fluorescence. These results show that a substantial portion of the folate receptor is present in the same endocytic compartments as the transferrin receptor.

Ultrastructural identification of Tf- and DAF-containing subcellular compartments was accomplished using colloidal gold probes (Figure 5). Tf-containing compartments were marked by incubating cells with diferric fluorescein isothiocyanate (FITC)-Tf conjugated to 6 nm colloidal gold particles (FITC-Tf–Au-6) which was shown to recycle similarly to Cy3-Tf. For electron microscopy, TRVb-1 cells or DAFTb-1 cells were loaded with FITC-Tf–Au-6 for 90 min at 37°C in the presence of 3 µg/ml anti-DAF monoclonal antibody and preserved for cryo-ultramicrotomy. Anti-DAF antibody was localized with rabbit anti-mouse polyclonal antiserum followed by protein A conjugated with 15 nm colloidal gold (protein A–Au-15). Protein A–Au-15 was not observed in thin sections (110 nm) of TRVb-1 cells treated with the anti-DAF antibody but stained both the cell surface and intracellular compartments in DAF-expressing cells treated with the anti-DAF antibody. Most of the internalized transferrin and DAF were localized in compartments that were <100 nm in diameter (Figure 5D), and many of them were tubular or tubulo-vesicular in shape (Figure 5A–C). The morphology of these structures is consistent with the morphology of the endocytic recycling compartment (Tooze and Hollinshead, 1991; Marsh *et al.*, 1995). Only a subset of the labeled organelles contained both labeled Tf and DAF (Figure 5C and D). This may be due to the low number of gold particles per vesicle profile which makes it unlikely that labeling with both types of gold will be seen in a single organelle. Some images of small tubulo-vesicular complexes revealed FITC-Tf–Au-6 and protein A–Au-15 in apparently unconnected compartments (e.g. Figure 5A). We cannot tell from electron microscopy if these are actually connected parts of the endocytic recycling compartment or separate compartments that are in close proximity. Protein A–Au-15 staining was also found in multivesicular compartments as well as other large membrane profiles (Figure 5C, inset).

Cholesterol depletion accelerates the export rates of GPI-anchored proteins

To determine the effect of cholesterol depletion on the trafficking of GPI-anchored proteins, FRαTb-1 cells were treated with lipoprotein-depleted serum and compactin, an inhibitor of HMG-CoA synthetase, to reduce exogenous and endogenous sources of cholesterol. The cells were incubated in the presence of small amounts of mevalonate
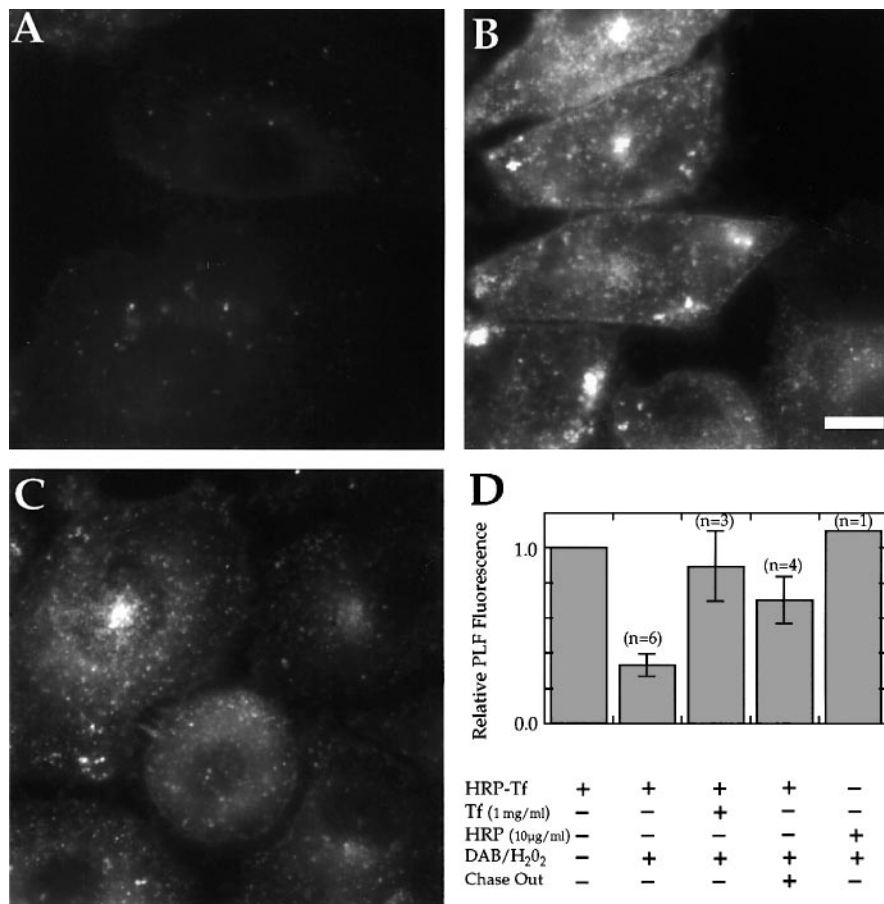
Fig. 4. Co-localization of folate receptors with HRP-Tf. FRαTb-1 cells were incubated with 10 nM PLF for 140 min at 37°C, and then incubated with HRP-Tf (**A**), pre-pulsed with 0.5 mg/ml HRP for 1 h and chased for 3 h in the presence of PLF (**B**), or incubated with HRP-Tf in the presence of 100-fold excess unlabeled transferrin (**C**) for an additional 40 min, and processed for DAB cytochemistry as described in Materials and methods. PLF fluorescence images were obtained as described. Quantitative analyses (**D**) of PLF for the conditions indicated were carried out as described in Materials and methods. PLF fluorescence in each case was normalized to the untreated samples. Bar = 10 µm.

to allow the synthesis of essential metabolites of mevalonate (Ryan *et al.*, 1981). Compactin-treated cells had 36.8 ± 3.5 nmol cholesterol/mg cell protein compared with untreated or cholesterol-replete cells which had 67 ± 3.5 nmol cholesterol/mg cell protein (Figure 6A). The phospholipid levels in these cells were relatively unaffected (data not shown).

The rate of export of C_6-NBD-SM was relatively unchanged in cells depleted of cholesterol compared with cells grown in the presence of control complete medium: the rate constants for exit of C_6-NBD-SM are 0.075 and 0.061/min in control and cholesterol-depleted cells, respectively (Figure 6B; Table I). As an additional control, we measured the rate of export of a transferrin receptor with a truncated cytoplasmic domain (Δ3-59-TfR; McGraw *et al.*, 1991) in cholesterol-depleted cells and found that these proteins are also exported at rates comparable with that measured in cholesterol-replete cells (Table I).

In contrast, reduction in cholesterol levels resulted in a dramatic increase in the export rates of the GPI-anchored proteins: the rate constants for export of the folate receptor and DAF were 0.075/min and 0.061/min, respectively (Figure 7A and C), indistinguishable from the export rate constants of C_6-NBD-SM and recycling receptors (Table I). Measurement of the extent of intracellular sequestration of GPI-anchored proteins showed that cholesterol depletion

also caused a drastic reduction in the fraction of GPI-anchored proteins that were intracellular (Figure 7B and D; Table I). After cholesterol depletion at steady state, only ~29% of the folate receptor and ~26% of DAF are found inside the cell. A similar reduction in intracellular folate receptors was observed following treatment with lovastatin (not shown). The reduction in intracellular levels of GPI-anchored proteins can be reversed by the inclusion of exogenous low density lipoprotein (LDL) in the presence of compactin for 16 h, showing that cholesterol levels in cell membranes are responsible for reduction in the intracellular pool of GPI-anchored proteins (Figure 7B).

To confirm that cholesterol depletion did not grossly alter the intracellular trafficking pathway of the GPI-anchored proteins, exogenously added PLF was co-internalized with Cy3-Tf. Figure 8 shows that after cholesterol depletion the internal folate receptor pools are still co-localized with internalized Tf. Similar results were obtained when DAF-expressing cells were depleted of cholesterol; the internalized pool of DAF was co-localized extensively with internalized transferrin.

Internalization of GPI-anchored proteins is unaffected by cholesterol depletion

As described in Materials and methods, the rates of internalization of the folate receptor and DAF in CHO
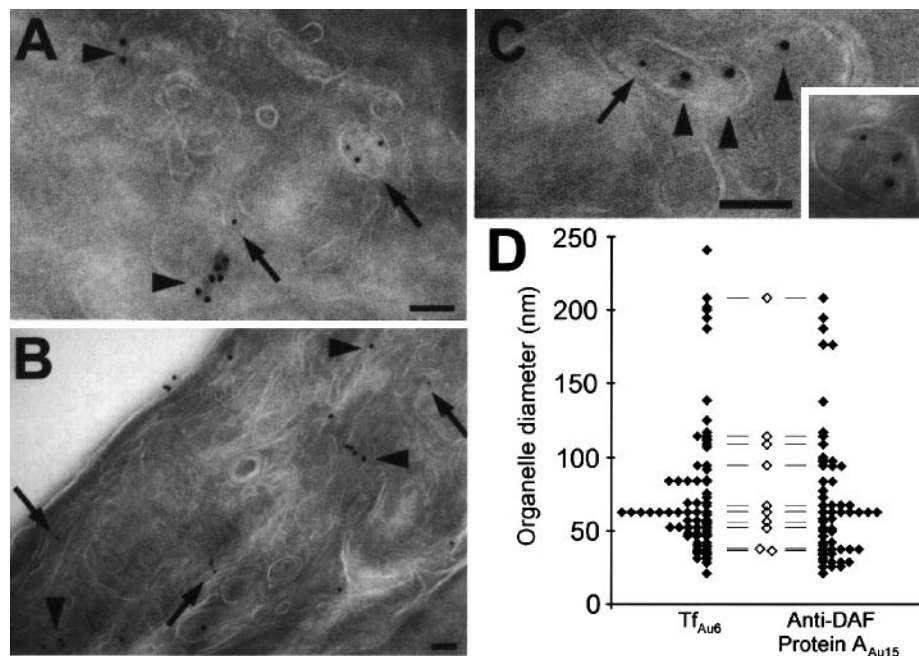
Fig. 5. Ultrastructural localization of DAF and transferrin. (**A–C**) DAFTb-1 cells were incubated with FITC-Tf–Au-6 (arrows) and anti-DAF which was detected by protein A–Au-15 (arrowheads). Both transferrin and DAF were found in similar intracellular compartments which were mainly small vesicles and tubular structures (A and B). Some of these tubules were labeled with both markers (C). Occasionally, multivesicular compartments were observed containing transferrin and DAF (C, inset). (**D**) A quantitative analysis of the diameter of organelles containing transferrin and anti-DAF was carried out. The smallest diameter of each organelle containing a gold particle was measured, and each filled symbol represents one organelle. Organelles containing both transferrin and DAF are shown by open symbols. Bars = 100 nm.

cells can be calculated from the externalization rates and the surface to internal ratios with the assumption that both internalization and externalization are described by single first order rate processes. Table I shows that cholesterol depletion does not significantly affect internalization rate constants and that these rates are similar to the rate of bulk membrane internalization measured in many different fibroblast lines. For example, the k_i for folate receptor and DAF are close to the k_i for Δ3-59-TfR expressed in TRVb cells (McGraw *et al*., 1991; Johnson *et al*., 1993).

Discussion

Internalization of GPI-anchored proteins
There is considerable uncertainty regarding the means of internalization of GPI-anchored proteins, which resemble phospholipids with a large proteinaceous head group. Since GPI-anchored proteins in their native state are distributed diffusely at the cell surface in many different cell types (Mayor *et al*., 1994; Parton *et al*., 1994; Mayor and Maxfield, 1995), it seems likely that they are internalized non-selectively, via clathrin-coated and non-coated invaginations (Lamaze and Schmid, 1995; Mukherjee *et al*., 1997). In support of this, we have found, using fluorescently labeled reagents (PLF and anti-DAF Fab), that GPI-anchored proteins are endocytosed at overall rates that are indistinguishable from rates of internalization of a modified transferrin receptor that lacks a functional internalization motif (Table I). This is similar to other membrane proteins lacking functional endocytosis signals which are internalized 5–20 times more slowly than proteins with intact signals (Trowbridge *et al*., 1993).

In our assays, we did not measure internalization rates directly, but we measured the surface to internal ratio at steady state and the rate of delivery of recycling receptors to the cell surface. As described in the Materials and methods, the internalization rate can be inferred from such measurements if the internalization and externalization are both first order kinetic processes. The data on externalization of folate receptors and DAF are all consistent with a single first order rate process. It is possible that our measurements would miss a rapidly equilibrating endocytic recycling process, and in that case our measurements would report net internalization after equilibration of the fast recycling. However, we could detect no evidence for such a fast process. Furthermore, the rates of internalization that we determined for MA104 cells are not very different from the values obtained using [³H]folate in an internalization assay (Chang *et al*., 1992).

Cholesterol-dependent sorting of GPI-anchored proteins in the endocytic pathway
Similar to other cell surface molecules, internalized GPI-anchored proteins are delivered rapidly to early sorting endosomes wherein recycling components (e.g. the transferrin receptor or the LDL receptor) are sorted from lysosomally directed components (e.g. acid-released ligands such as LDL or α₂-macroglobulin). From our studies, we cannot exclude the possibility that GPI-anchored proteins are delivered to sorting endosomes via parallel endocytic pathways (Lamaze and Schmid, 1995), different from the pathway of receptor-mediated endocytosis. However, our data as well as other electron microscopic studies (Birn *et al*., 1993; Rijnboutt *et al*., 1996) show that internal GPI-anchored proteins are mainly in endosomes.

We have shown that after internalization, C₆-NBD-SM and related fluorescent lipid analogs transit the endocytic

A

B
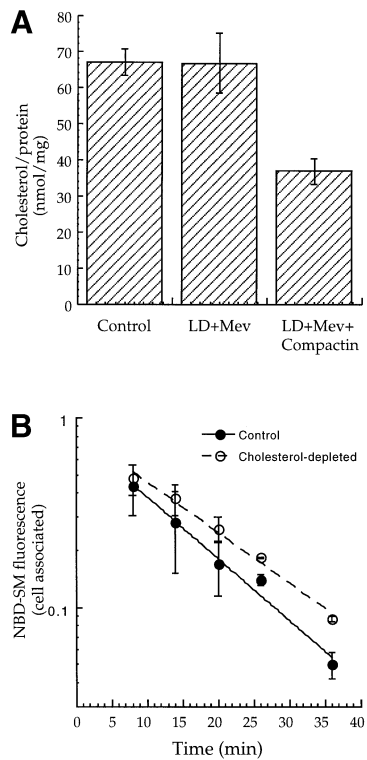
Fig. 6. C_6-NBD-SM recycling is unaffected by cholesterol depletion. (**A**) Cholesterol levels in FRαTb-1 cells grown with or without compactin for 4 days. After growing the cells under the indicated conditions, cholesterol levels in the cells were analyzed. Control, cells incubated with complete medium (folate-free F-12 with 5% fetal bovine serum); LD+Mev, cells grown in lipoprotein-deficient serum in the presence of 200 μM mevalonic acid; LD+Mev+Compactin, cells grown in LD+Mev in the presence of 10 μM compactin. Error bars represent standard deviation of the mean from two separate dishes. (**B**) Recycling of C_6-NBD-SM in cholesterol-depleted and control cells. FRαTb-1 cells were grown under control conditions (●) or with LD+Mev+Compactin (○) as described above and labeled with C_6-NBD-SM. Following a 10 min pulse, the rate of export of internalized C_6-NBD-SM during the chase period was determined as described in Materials and methods. The curves were fit to a first order exponential by the method of least squares. The two equations with the best fit ($R > 0.99$) are $y = 0.81 \times e^{-0.075t}$ and $y = 0.85 \times e^{-0.061t}$ for the control and compactin-treated conditions, respectively. Error bars represent standard deviation of the mean values from two separate dishes.

system in a way that is kinetically and morphologically indistinguishable from recycling receptors. These data have provided evidence for a default recycling pathway for membrane proteins and lipid (Dunn *et al.*, 1989; Mayor *et al.*, 1993). These data also imply that retention of membrane proteins in the endocytic pathway should require specific sorting mechanisms.

GPI-anchored proteins, although lacking cytoplasmic domains, are recycled at a 3-fold slower rate than C_6-NBD-SM or transferrin receptors (Table I). This retardation in export rates leads to a dramatic intracellular accumulation of GPI-anchored proteins (50% of the recycling pool), revealing a novel function for the GPI-anchoring of proteins. This intracellular retention of GPI-anchored proteins is regulated by the levels of cholesterol in the membrane since GPI-anchored proteins are trafficked with the same kinetics and via the same pathways as other recycling components in cells depleted of cholesterol (Figure 8; Table I).

Lipid-dependent traffic of proteins has been observed previously. For example, in the biosynthetic pathway in yeast, sphingolipid levels modulated the egress of GPI-anchored proteins out of the endoplasmic reticulum (Sutterlin *et al.*, 1997), and in MDCK cells the inhibition of sphingolipid biosynthesis resulted in a general loss of polarized delivery to the apical cell surface (Mays *et al.*, 1995). In addition, it has been shown recently that cholesterol depletion in MDCK cells results in the missorting of an apically delivered protein, hemagglutinin, and possibly a GPI-anchored protein (Keller and Simons, 1998). These observations are consistent with the involvement of raft-dependent mechanisms for the apical sorting and transport of a select class of proteins in the biosynthetic pathway (Simons and Ikonen, 1997). The influence of cholesterol levels on the retention of GPI-anchored proteins in endosomes strongly suggests that these mechanisms are also involved in the sorting of GPI-anchored proteins in endosomes. Consistent with this, we have found recently that depletion of sphingolipid levels in FRαTb-1 cells also accelerates the recycling of GPI-anchored proteins similarly to that observed under cholesterol depletion conditions (S.Chatterjee, E.Smith, V.L.Stevens and S.Mayor, in preparation), and that GPI-anchored proteins occur in cholesterol-dependent sub-micron domains in cell membranes (Friedrichson and Kurzchalia, 1998; Varma and Mayor, 1998).

Implications for GPI-anchored protein function
The major site for intracellular accumulation of GPI-anchored proteins is the peri-centriolar endocytic recycling compartment. However, following endocytosis, the GPI-anchored proteins are distributed somewhat more peripherally than transferrin receptors. This suggests that GPI-anchored proteins may be retained in sorting endosomes to some extent. Since sorting endosomes become maturing endosomes or endosome carrier vesicles with a $t_{1/2}$ of 8–10 min (Dunn and Maxfield, 1992; Gruenberg and Maxfield, 1995), this retention would cause some GPI-anchored proteins to reach late endosomes. Delivery of some folate receptors to late endosomes is supported by an electron microscopic study which showed that the entire endocytic pathway, including both early and late endosomes, contains immunoreactive folate receptors (Rijnboutt *et al.*, 1996). Our electron microscopy immunolocalization of internalized DAF also showed delivery to multivesicular bodies.

The ability of GPI-anchored proteins to be sorted from bulk membrane in endosomes has significant implications for GPI anchor function. The retention in endosomes will expose these proteins to the acidic milieu of both sorting and recycling endosomes for longer times than recycling receptors with conventional transmembrane tails. Furthermore, this retention may take place in specialized membrane domains (Simons and Ikonen, 1997). GPI-anchored cellular scrapie protein is processed to the infectious proteinase K-resistant prion form more efficiently than a form of the scrapie protein with a transmembrane peptide anchor. This processing is dependent on acidic pH in endosomes and is inhibited by the depletion of cholesterol in membranes (Taraboulos *et al.*, 1995). We propose that
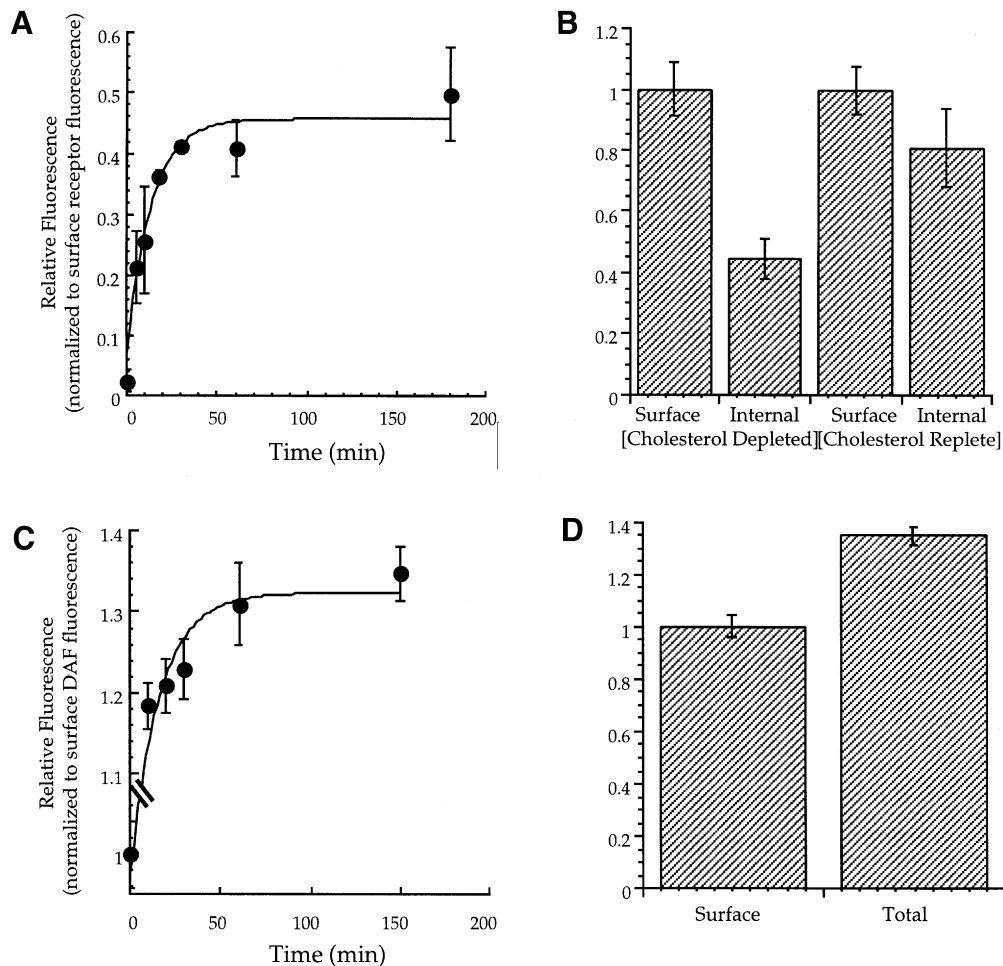
Fig. 7. Trafficking kinetics of GPI-anchored proteins in cholesterol-depleted cells. (**A**) FRαTb-1 cells were depleted of cholesterol, and the rate of export of the folate receptor was determined exactly as described in Figure 1C. The data shown are an average of two independent experiments. The points were fitted to a curve $y = 0.05 + 0.38 \times [1 - e^{(-0.075t)}]$ by the method of least squares ($R = 0.98$). Error bars in all panels represent standard errors from the weighted means. (**B**) FRαTb-1 cells were depleted of cholesterol (Cholesterol depleted) or first depleted and then replenished with a cholesterol source, LDL (20 μg/ml), for 16 h in the presence of lipoprotein-deficient serum and compactin (Cholesterol replete). The surface and internal receptors were then quantified as described in Figure 1B. Each data point is an average of two independent experiments. (**C**) DAFTb-1 cells were depleted of cholesterol, and the rate of export of DAF was determined exactly as described in Figure 1D. The data shown are an average of two independent experiments. The points were fitted to a curve $y = 1 + 0.35 \times [1 - e^{(-0.061t)}]$ by the method of least squares ($R = 0.97$). (**D**) DAFTb-1 cells were depleted of cholesterol and the surface and internal pools of DAF were then quantified as described in Figure 1D. Each data point is an average of two independent experiments.

the GPI anchor causes retention of the cellular scrapie protein in acidic endosomes which would be lost with a transmembrane anchor. This cholesterol-dependent retention mechanism could facilitate the efficient conversion of native scrapie protein into prions, possibly in distinct membrane domains or aggregates.

It has been proposed that GPI-anchored proteins such as the folate receptor take up small molecules in caveolae via a process called potocytosis which involves the transient closure of cell surface caveolae containing clustered folate receptors and other molecules, during which the caveolae are acidified and the receptors release their ligands into the caveolar lumen (Anderson, 1993). This would increase the effective concentration of the released folate molecules several fold, thereby facilitating the ability of folate transporters to transfer folate across the cell membrane. We propose, instead, that it is the retention/ sorting of the GPI-anchored folate receptor in acidic endosomes which increases the local concentration of GPI-anchored folate receptors in endosomes for efficient

delivery of folate to the cytoplasm. This would also make the GPI-anchored folate receptors more efficient in folate uptake than the protein-anchored form (Ritter *et al.*, 1995). Furthermore, our data also provide an explanation for the drastic reduction in folate uptake efficiency in cells depleted of cholesterol (Rothberg *et al.*, 1990a; Chang *et al.*, 1992).

Conclusion

In this report, we demonstrate a novel function of GPI anchoring of proteins, namely, retention in endosomes. This has important implications for the biology of some GPI-anchored proteins. We provide evidence that the ability of GPI-anchored proteins to sort from bulk membrane proteins and lipids in a manner dependent on the cholesterol content of membranes provides greater access to specialized environments in endosomes, and this sorting may be functionally significant. Finally, our data are consistent with the involvement of raft-dependent mechanisms for the sorting of GPI-anchored proteins in endosomes.

previously (Dunn and Maxfield, 1992). HRP was obtained from Bangalore Genei (Bangalore, India). All chemicals were from Sigma and tissue culture supplies were from Gibco-BRL (Gaithersburg, MD) unless otherwise specified.

Cells and cell culture
CHO cell lines were maintained in Hams F-12 medium supplemented with 5% fetal bovine serum (FBS), 100 U/ml penicillin and 100 μg/ml streptomycin unless otherwise specified. DAF-expressing CHO cells (DAFTb-1 cells) and folate receptor-expressing CHO cells (FRαTb-1 cells) were derived from the human transferrin receptor-expressing CHO line, TRVb-1, as described previously (Mayor and Maxfield, 1995). FRαTb-1 cells were maintained in folate-free Ham's F-12 medium (Specialty Media, Lavallette, NJ) with 5% FBS, 100 μg/ml geneticin and 200 μg/ml hygromycin (Calbiochem). MA104 cells, a monkey kidney epithelial cell line, were maintained in folate-deficient RPMI (Specialty Media) with 5% FBS and plated 5 days prior to the experiment in folate-deficient RPMI containing 5% dialyzed FBS. The specificity and phosphatidylinositol-specific phospholipase C (PI-PLC) sensitivity of fluorescence labeling of the folate receptors in FRαTb-1 cells with PLF, and DAF in DAFTb-1 cells with Cy3-anti-DAF Fab fragments have been described previously (Mayor and Maxfield, 1995).

Cholesterol depletion
Cells were grown for 4 days in 5% lipoprotein-deficient serum with 200 μM mevalonate and 5–10 μM compactin to deplete cholesterol stores (Rothberg et al., 1990a). In some experiments, 10 μM lovastatin was used instead of compactin. Cholesterol-replete cells were grown either in medium containing 5% lipoprotein-deficient serum with 200 μM mevalonate and 25 μg/ml exogenous human LDL or in 5% complete serum with similar results.

Sterol analyses and membrane recycling assays
Cholesterol and lipid phosphorus were assayed in cells grown in 6-well plates as described previously (Tabas et al., 1985). Compactin (10 μM) was included in all incubation buffers that were used with cells depleted of cholesterol. Membrane export rates in cholesterol-replete and depleted cells were determined using C_6-NBD-SM as a membrane marker in biochemical experiments as described previously (Mayor et al., 1993; Presley et al., 1993).

Kinetics assays
The efflux kinetics of the different GPI-anchored proteins were obtained in an assay used previously to measure the exocytic rate constant of transferrin receptors (Johnson et al., 1993). Cells were incubated in the presence of saturating amounts of ligand until they achieved a steady state value at 37°C. In the presence of saturating ligand, the amount of surface-bound ligand (L·R_s) can be treated as a constant because relative to the time course of the assay, the binding of PLF to folate receptors and mAbs (1A10 or F1A10) to DAF is relatively rapid even at 0°C (half-maximal binding is observed in <5 min at 0°C in both cases). The total number of occupied receptors (L·R_t) is thus a sum of this constant and the ligand bound to the receptors inside the cells (L·R_i).

$$L·R_t = L·R_s + L·R_i \tag{1}$$

The rate of accumulation of ligand-bound receptors is thus dependent on the rate at which unoccupied receptors arrive at the cell surface and is equal to the rate of loss of unoccupied internal receptors. This may be described by the following first order rate equation

$$L·R_i = L·R_{i,ss}×[1 - e^{(-k_e t)}] \tag{2}$$

where L·R_i is the amount of internal ligand-bound receptor at time t, and L·$R_{i,ss}$ is the total ligand-bound receptors at steady state. Combining equations 1 and 2,

$$L·R_t = L·R_s + L·R_{i,ss}×[1 - \exp^{(-k_e t)}] \tag{3}$$

The values for k_e are determined as the values for the best fit to this function where the values for L·$R_{i,ss}$, L·R_t, and k_e are fit by a least squares analysis.

The rate of internalization of ligand-bound receptors may be described by the following differential equation

$$dL·R_i = L·R_s×k_i \, dt - L·R_i×k_e \, dt \tag{4}$$

Fig. 8. Endocytic pathway of folate receptors in cholesterol-depleted FRαTb-1 cells. FRαTb-1 cells were depleted of cholesterol as described in Materials and methods. The cells were then incubated with 10 nM PLF (**A**) and 5 μg/ml Cy3-Tf (**B**) for 3 h at 37°C and processed for microscopy. PLF fluorescence (A) and Cy3-transferrin (B) were imaged by digital fluorescence microscopy and printed using identical contrast settings. Arrows indicate peripheral endosomes, and arrowheads indicate central recycling compartments. Bar = 10 μm.

Materials and methods

Materials
Mouse mAb to the human folate receptor (MOv19; Coney et al., 1991) was a gift from Dr Richard Anderson and Centocor Corp. (Malvern, PA). Species-specific polyclonal IgGs to primary antibodies were obtained from Pierce Chemical Co. (Rockford, IL). Mouse mAb to DAF, 1A10 (Davitz et al., 1986), was a gift from M.Davitz (New York University). Fab fragments of mAb 1A10 were generated according to published procedures (Howard and Lane, 1988) and found to be free of contaminating intact antibody. Labeling of mAbs, Fab fragments and transferrin with the fluorophore Cy3 (Biological Detection Systems, Inc., Pittsburgh, PA) or fluorescein succinimidyl ester (Molecular Probes, OR) was carried out according to the manufacturer's instructions. PLF (McAlinden et al., 1991) was obtained from Dr J.Hynes (Medical University of South Carolina). Poly-D-lysine-treated coverslip bottom dishes were made and used for growing cells for all microscopy studies as previously described (Mayor et al., 1993). C_6-NBD-SM from Molecular Probes was purified by thin layer chromatography before use. Fluorescein-labeled dextran (10 kDa; F-Dex) was obtained from Molecular Probes, Inc. and used after extensive dialysis. Lipoprotein-deficient serum was prepared as described (Pitas et al., 1981). Compactin (mevastatin) from Sigma (St. Louis, MO) was converted to its sodium salt as previously described (Ryan et al., 1981). The sodium salt of lovastatin and human LDL were kindly supplied by Dr Ira Tabas (Columbia University, NY). DiI-labeled LDL was prepared as described

where k_i is the first order internalization rate constant. At steady state $dL \cdot R_i / dt = 0$, therefore

$$k_i = \frac{L \cdot R_{i,ss} \times k_e}{L \cdot R_s} \qquad (5)$$

Cell labeling

To determine $L \cdot R_s$, $L \cdot R_i$ and $L \cdot R_t$ in MA104 and DAFTb-1 cells, the following protocols were followed. MA104 cells were incubated in the presence of 20 nM PLF in folate-free Hams F-12 medium (F^- HF) supplemented with 1 mg/ml chicken ovalbumin and 4.5 g/l HEPES pH 7.4 (F^- HF-ova) at 0 or 37°C for various lengths of time, and rinsed in ice-cold medium 1 (150 mM NaCl, 5 mM KCl, 1 mM CaCl$_2$, 1 mM MgCl$_2$, 20 mM HEPES pH 7.4). The cells were then incubated for 30 min at 0°C in ice-cold F^- HF-ova containing 4 µg/ml Cy3-labeled mAb to the folate receptor (Cy3-MOv19) (to normalize for the number of surface receptors per field). DAFTb-1 cells were pre-incubated in F-12 medium supplemented with 0.2% bovine serum albumin (BSA), 1.2 g/l glucose and 4.5 g/l HEPES pH 7.4 (HF-BSA) for 10 min at 37°C. The cells were then incubated for various lengths of time at 0 or 37°C with Cy3-labeled Fab fragment (Cy3-anti-DAF) at 20 µg/ml. The cells were rinsed in ice-cold medium 1 and incubated with fluorescein-labeled goat anti-mouse IgG (F-GAM; 100 µg/ml) at 0°C for 30 min (to normalize for surface receptor expression per field), rinsed and taken for fluorescence imaging. Control incubations were performed with an irrelevant mouse mAb at 20 µg/ml or with DAFTb-1 cells which had been treated with PI-PLC for 3 h prior to labeling with Cy3-anti-DAF. The level of fluorescence observed in these control incubations was <5% of the average signal obtained in a surface-binding assay.

In some experiments with FRαTb-1 cells, the internal pool of receptors ($L \cdot R_i$) was determined directly by pre-incubating the cells with folic acid (20 nM) for 1 h at 0°C to block surface-exposed folate receptors, before incubation with PLF at 37°C for various periods to label the newly externalized receptors directly. The surface receptors ($L \cdot R_s$) in the same experiment were quantified separately by incubating cells at 0°C with PLF. The extent of binding of PLF at 0°C to folic acid-incubated cells was <5% of the PLF fluorescence obtained under surface-binding conditions.

The extent of combined autofluorescence and non-specific PLF binding to the cells at 37°C was measured in the presence of 500-fold excess folic acid (10 µM). In FRαTb-1 cells, the non-specific values were <5% of the surface fluorescence values. For MA104 cells, non-specific fluorescence was between 5 and 14% of the surface-binding values.

All the cells were rinsed at room temperature in a high potassium buffer (120 mM KCl, 5 mM NaCl, 1 mM CaCl$_2$, 1 mM MgCl$_2$) in the presence of 10 µM nigericin before quantitative fluorescence microscopy to collapse the endosomal pH gradients.

Fluorescence microscopy and quantitative analyses

Fluorescence microscopy and digital image collection were performed using a Leitz Diavert fluorescence microscope equipped with a Photometrics (Tucson, AZ) cooled CCD camera and driven by software from Inovison Corp. (Durham, NC) as described previously (Mayor et al., 1993). In some instances, fluorescence images were collected using a Nikon TMD fluorescence microscope equipped with a Princeton Instruments (Princeton, NJ) cooled CCD camera driven by Metamorph software (Universal Imaging Corporation, West Chester, PA). For output purposes, the digital images were intensity mapped through logarithmic look up tables (luts).

Fluorescence quantification was carried out with a low magnification objective (25×, NA 0.8) to obtain 30–100 cells per field, while the images for visualization purposes were obtained with a 63×, NA 1.4 objective. For the efflux assays, a phase contrast image and two fluorescence images with fluorescein and rhodamine optics were obtained for each field as described earlier (Mayor et al., 1993).

Total fluorescence per field was obtained by summing the pixel intensity over the whole field after subtracting a background image obtained from six to eight fields that did not contain any cells. Images including autofluorescence and non-specific fluorescence were obtained under the same illumination and exposure conditions, and these were used to determine appropriate threshold criteria to determine the total fluorescence per field. Because of the cell to cell variability in receptor expression, the PLF fluorescence per field and Cy3-anti-DAF fluorescence per field were corrected for the total surface receptors per field. Cy3-MOv19 was used to detect surface folate receptors and F-GAM was used to detect anti-DAF present at the surface of cells at the end of the

incubations, thereby providing a normalization factor proportional to the total surface receptors per field. The fluorescence from each of the fields was normalized using this factor. A mean value and standard deviation were obtained from 9–11 fields per dish. The mean values, µ1 and µ2, and deviations, σ1 and σ2, from the two independent determinations (two dishes per data point of a single experiment) were combined and represented as a weighted mean µ of these two independent determinations.

Horseradish peroxidase-dependent fluorescence quenching

HRP was conjugated to iron-loaded transferrin using sodium metaperiodate. Briefly, 2 mg of HRP in 400 µl of water was reacted with 0.1 ml of 0.1 M sodium metaperiodate for 20 min at room temperature. HRP was separated from the reaction mixture by passing through a 2 ml Sephadex G-25 column with 1 mM sodium acetate buffer, pH 4.5. Transferrin (2 mg) was mixed with oxidized HRP in 0.1 M sodium carbonate buffer, pH 9.5 and incubated at room temperature for 2 h in a final volume of 1 ml. Then 0.1 ml of a freshly prepared 4 mg/ml solution of sodium borohydride was added to the reaction mixture, and it was incubated further at 4°C for 2 h. The reaction mixture was then dialyzed against phosphate-buffered saline (PBS), pH 7.2. The mixture was fractionated by FPLC using a Superose 6 gel filtration column (Pharmacia, Sweden), and the fractions were analyzed on an 8% polyacrylamide gel. Conjugate fractions corresponding to approximate mol. wts of 120–160 kDa were pooled and used as HRP-Tf in the fluorescence quenching assay. These conjugate species have 1–2 HRP molecules per molecule of transferrin.

To measure the extent of overlap between the folate receptor and transferrin receptor in endosomes, FRαTb-1 cells were incubated with 20 nM PLF for 3 h at 37°C, and in the last 40 min of incubation HRP-Tf (10 µg/ml) was added to label the endocytic recycling pathway. For some experiments, excess transferrin (1 mg/ml) was added to block uptake of HRP-Tf. In separate dishes, PLF-labeled cells were incubated with HRP (0.5 mg/ml) for 1 h and chased for 3 h to deliver HRP to late endosomes and lysosomes. In one experiment (Figure 4D, Chase Out), HRP-Tf was present only during the first 40 min of the 3 h incubation with PLF. At the end of the labeling reactions, the cells were cooled on ice and washed twice with ice-cold medium 1–5 min each. The cells were then washed four times (2 min each) with ice-cold citrate buffer (25 mM sodium citrate, 135 mM NaCl; pH 3.0) to strip surface-bound ligands. The cells were rinsed with medium 1 (two washes of 5 min each) and incubated with DAB (250µg/ml) and H$_2$O$_2$ (0.0025%) in the dark for 30 min on ice. Excess DAB and H$_2$O$_2$ were rinsed off with two washes of medium 1 (5 min each), and the cells were processed for fluorescence microscopy. To label only the surface with HRP-Tf, some cells were incubated with HRP-Tf for 30 min on ice after completion of steady-state PLF labeling and acid rinses.

Ultrastructural immunolocalization of transferrin and DAF

TRVb-1 cells or DAFTb-1 cells were incubated in culture medium with 5 µM deferoxamine for 24 h prior to the experiment. Cells were incubated for 90 min at 37°C with a combination of FITC–transferrin coupled to 6 nm colloidal gold [FITC-Tf–Au-6; prepared as described in Marsh et al. (1995)] and 3 µg/ml monoclonal anti-DAF (clone 1A10) in 1% BSA in Ham's F-12 medium. The correct trafficking of FITC-Tf–Au-6 as a ligand for the transferrin receptor was validated as described previously (Marsh et al., 1995). Following the incubation, cells were fixed with 4% paraformaldehyde, 0.5% glutaraldehyde in a 1:1 mixture of medium 1 and 200 mM HEPES, pH 7.4 for 15 min at room temperature. Cells were removed from the plastic culture dish by scraping, centrifuged at 1000 g, overlaid with fresh fixative, and maintained at 4°C overnight. Cell pellets were infused with 1.2 M sucrose in sodium phosphate buffer for 30 min, 2.3 M sucrose in phosphate buffer for 30 min, mounted on aluminum pins, and frozen in liquid nitrogen. Thin sections (110 nm) were cut at –80°C using an RMC MT7 ultramicrotome equipped with an RMC CR21 cryobox attachment and transferred to grids (Tokuyasu, 1973). Immunogold staining was performed essentially as described (Griffiths, 1993). Grids were treated with 1% BSA, 5% goat serum, 0.12% glycine in PBS, pH 7.4 ('blocking solution') for 20 min and then transferred to blocking solution containing 1:100 dilution of rabbit anti-mouse IgG polyclonal antibody (Cappel, Inc.) for 30 min. Grids were washed once with 1% BSA/PBS, and three times in PBS before application of protein A conjugated with 15 nm colloidal gold (J.Slot, Utrecht) in 1% BSA/PBS for 30 min, washed once in 1% BSA/PBS, three times with PBS, stabilized with 0.1% glutaraldehyde in PBS (5 min), exchanged with distilled water, counterstained with a 1:10 dilution of saturated aqueous

uranyl acetate in 2% methylcellulose for 10 min, air dried in 3.5 mm nichrome loops (Electron Microscopy Sciences, Inc.), and observed using a JEOL 100 CX II transmission electron microscope operating at 80 keV.

Acknowledgements

References

Anderson,R.G.W. (1993) Potocytosis of small molecules and ions by caveolae. *Trends Cell Biol.*, **3**, 69–72.

Angelov,D.N., Gunkel,A., Stennert,E. and Neiss,W.F. (1995) Phagocytic microglia during delayed neuronal loss in the facial nucleus of the rat: time course of the neuronofugal migration of brain macrophages. *Glia*, **13**, 113–129.

Birn,H., Selhub,J. and Christensen,E.I. (1993) Cell fractionation and electron microscope studies of kidney folate-binding protein. *Am. J. Physiol.*, **264**, C302–C310.

Borchelt,D.R., Taraboulos,A. and Prusiner,S.B. (1992) Evidence for synthesis of scrapie prion proteins in the endocytic pathway. *J. Biol. Chem.*, **267**, 16188–16199.

Brown,D. (1993) The tyrosine kinase connection: how GPI-anchored proteins activate T cells. *Curr. Opin. Immunol.*, **5**, 349–354.

Chang,W.-J., Rothberg,K.G., Kamen,B.A. and Anderson,R.G.W. (1992) Lowering cholesterol content of MA104 cells inhibits receptor-mediated transport of folate. *J. Cell Biol.*, **118**, 63–69.

Coney,L.R., Tomassetti,A., Carayannopoulos,L., Frasca,V., Kamen,B.A., Colnaghi,M.I. and Zurawski,V.J. (1991) Cloning of a tumor-associated antigen: MOv18 and MOv19 antibodies recognize a folate-binding protein. *Cancer Res.*, **51**, 6125–6132.

Davitz,M.A., Low,M.G. and Nussenzweig,V. (1986) Release of decay-accelerating factor (DAF) from the cell membrane by phosphatidylinositol-specific phospholipase C (PIPLC): selective modification of a complement regulatory protein. *J. Exp. Med.*, **163**, 1150–1161.

Dunn,K.W. and Maxfield,F.R. (1992) Delivery of ligands from sorting endosomes to late endosomes occurs by maturation of sorting endosomes. *J. Cell Biol.*, **117**, 301–310.

Dunn,K.W., McGraw,T.E. and Maxfield,F.R. (1989) Iterative fractionation of recycling receptors from lysosomally destined ligands in an early sorting endosome. *J. Cell Biol.*, **109**, 3303–3314.

Dupree,P., Parton,R.G., Raposo,G., Kurzchalia,T.V. and Simons,K. (1993) Caveolae and sorting in the *trans*-Golgi network of epithelial cells. *EMBO J.*, **12**, 1597–1605.

Ferguson,M.A.J. (1994) What can GPI do for you. *Parasitol. Today*, **10**, 48–52.

Field,M.C. and Menon,A.K. (1992) Glycolipid-anchoring of cell surface proteins. In Schlesinger,M.J. (ed.), *Lipid Modification of Proteins*. CRC Press, Boca Raton, FL, pp. 83–134.

Friedrichson,T. and Kurzchalia,T.V. (1998) Microdomains of GPI-anchored proteins in living cells revealed by chemical cross-linking. *Nature*, in press.

Fujimoto,T. (1996) GPI-anchored proteins, glycosphingolipids and sphingomyelin are sequestered to caveolae only after crosslinking. *J. Histochem. Cytochem.*, **44**, 929–941.

Griffiths,G. (1993) Fine structure immunochemistry. Springer-Verlag, Heidelberg, Germany, pp. 1–159.

Gruenberg,J. and Maxfield,F.R. (1995) Membrane transport in the endocytic pathway. *Curr. Opin. Cell Biol.*, **7**, 552–563.

Harder,T. and Simons,K. (1997) Caveolae, DIGs and the dynamics of sphingolipid-cholesterol microdomains. *Curr. Opin. Cell Biol.*, **9**, 534–542.

Hjelle,J.T., Christensen,E.I., Carone,F.A. and Selhub,J. (1991) Cell fractionation and electron microscope studies of kidney folate-binding protein. *Am. J. Physiol.*, **260**, C338–C346.

Howard,E. and Lane,D. (1988) *Antibodies: A Laboratory Manual*. Cold Spring Harbor Laboratory Press, Cold Spring Harbor, NY.

Johnson,L.S., Dunn,K.W., Pytowski,B. and McGraw,T.E. (1993) Endosome acidification and receptor trafficking: bafilomycin A1 slows receptor externalization by a mechanism involving the receptor's internalization motif. *Mol. Biol. Cell*, **4**, 1251–1266.

Kamen,B.A., Wang,M.T., Streckfuss,A.J., Peryea,X. and Anderson,R.G. (1988) Delivery of folates to the cytoplasm of MA104 cells is mediated by a surface membrane receptor that recycles. *J. Biol. Chem.*, **263**, 13602–13609.

Kamen,B.A., Johnson,C.A., Wang,M.T. and Anderson,R.G. (1989) Regulation of the cytoplasmic accumulation of 5-methyl-tetrahydrofolate in MA104 cells is independent of folate receptor regulation. *J. Clin. Invest.*, **84**, 1379–1386.

Keller,P. and Simons,K. (1998) Cholesterol is required for surface transport of influenza virus hemagglutinin. *J. Cell Biol.*, **140**, 1357–1367.

Keller,G.-A., Siegel,M.W. and Caras,I.W. (1991) Endocytosis of glycophospholipid-anchored and transmembrane forms of CD4 by different endocytic pathways. *EMBO J.*, **11**, 863–874.

Koval,M. and Pagano,R.E. (1989) Lipid recycling between the plasma membrane and intracellular compartments: transport and metabolism of fluorescent sphingomyelin analogues in cultured fibroblasts. *J. Cell Biol.*, **108**, 2169–2181.

Lamaze,C. and Schmid,S.L. (1995) The emergence of clathrin-independent pinocytic pathways. *Curr. Opin. Cell Biol.*, **7**, 573–580.

Lisanti,M.P., Caras,I.W., Gilbert,T., Hanzel,D. and Rodriguez,B.E. (1990) Vectorial apical delivery and slow endocytosis of a glycolipid-anchored fusion protein in transfected MDCK cells. *Proc. Natl Acad. Sci. USA*, **87**, 7419–7423.

Marsh,E.W., Leopold,P.L., Jones,N.L. and Maxfield,F.R. (1995) Oligomerized transferrin receptors are selectively retained by a lumenal sorting signal in a long-lived endocytic recycling compartment. *J. Cell Biol.*, **129**, 1509–1522.

Mayor,S. and Maxfield,F.R. (1995) Insolubility and redistribution of GPI-anchored proteins at the cell surface after detergent treatment. *Mol. Biol. Cell*, **6**, 929–944.

Mayor,S., Presley,J.P. and Maxfield,F.R. (1993) Sorting of membrane components from endosomes and subsequent recycling to the cell surface occurs by a bulk flow process. *J. Cell Biol.*, **121**, 1257–1269.

Mayor,S., Rothberg,K.G. and Maxfield,F.R. (1994) Sequestration of GPI-anchored proteins in caveolae triggered by cross-linking. *Science*, **264**, 1948–1951.

Mays,R.W., Siemers,K.A., Fritz,B.A., Lowe,A.W., van Meer,G. and Nelson,W.J. (1995) Hierarchy of mechanisms involved in generating Na/K-ATPase polarity in MDCK epithelial cells. *J. Cell Biol.*, **130**, 1105–1115.

McAlinden,T.P., Hynes,J.B., Patil,S.A., Westerhof,G.R., Jansen,G., Schornagel,J.H., Kerwar,S.S. and Freisheim,J.H. (1991) Synthesis and biological evaluation of a fluorescent analogue of folic acid. *Biochemistry*, **30**, 5674–5681.

McConville,M.J. and Ferguson,M.A. (1993) The structure, biosynthesis and function of glycosylated phosphatidylinositols in the parasitic protozoa and higher eukaryotes. *Biochem. J.*, **294**, 305–324.

McGraw,T.E., Pytowski,B., Arzt,J. and Ferrone,C. (1991) Mutagenesis of the human transferrin receptor: two cytoplasmic phenylalanines are required for efficient internalization and a second-site mutation is capable of reverting an internalization-defective phenotype. *J. Cell Biol.*, **112**, 853–861.

Mukherjee,S., Ghosh,R.G. and Maxfield,F.R. (1997) Endocytosis. *Physiol. Rev.*, **77**, 759–803.

Parton,R.G., Joggerst,B. and Simons,K. (1994) Regulated internalization of caveolae. *J. Cell Biol.*, **127**, 1199–1215.

Pitas,R.E., Innerarity,T.L., Weinstein,J.N. and Mahley,R.W. (1981) Acetoacetylated lipoproteins used to distinguish fibroblasts from macrophages *in vitro* by fluorescence microscopy. *Arteriosclerosis*, **1**, 177–185.

Presley,J.F., Mayor,S., Dunn,K.W., Johnson,L.S., McGraw,T.E. and Maxfield,F.R. (1993) The End2 mutation in CHO cells slows the exit of transferrin receptors from the recycling compartment but bulk membrane recycling is unaffected. *J. Cell Biol.*, **122**, 1231–1241.

Rijnboutt,S., Jansen,G., Posthuma,G., Hynes,J.B., Schornagel,J.H. and Strous,G.J. (1996) Endocytosis of GPI-linked membrane folate receptor-α. *J. Cell Biol.*, **132**, 35–47.

Ritter,T.E., Fajardo,O., Matsue,H., Anderson,R.G. and Lacey,S.W. (1995) Folate receptor targeted to clathrin-coated pits cannot regulate vitamin uptake. *Proc. Natl Acad. Sci. USA*, **92**, 3824–3828.

Robinson,P.J. (1991) Phosphatidylinositol membrane anchors and T-cell activation. *Immunol. Today*, **12**, 35–41.

Rothberg,K.G., Heuser,J.E., Donzell,W.C., Ying,Y.-S., Glenney,J.R. and Anderson,R.G.W. (1992) Caveolin, a protein component of caveolae membrane coats. *Cell*, **68**, 673–682.

Rothberg,K.G., Ying,Y.-S., Kamen,B.A. and Anderson,R.G.W. (1990a) Cholesterol controls the clustering of the glycophospholipid-linked membrane receptor for 5-methyltetrahydrofolate. *J. Cell Biol.*, **111**, 2931–2938.

Rothberg,K.G., Ying,Y.-S., Kolhouse,J.F., Kamen,B.A. and Anderson,R.G.W. (1990b) The glycophospholipid-linked folate receptor internalizes folate without entering the clathrin-coated pit endocytic pathway. *J. Cell Biol.*, **110**, 637–649.

Ryan,J., Hardeman,E.C., Endo,A. and Simoni,R.D. (1981) Isolation and characterization of cells resistant to ML236B (compactin) with increased levels of 3-hydroxy-3-methylglutaryl coenzyme A reductase. *J. Biol. Chem.*, **256**, 6762–6768.

Salzman,N.H. and Maxfield,F.R. (1988) Intracellular fusion of sequentially formed endocytic compartments. *J. Cell Biol.*, **106**, 1083–1091.

Simons,K. and Ikonen,E. (1997) Functional rafts in membranes. *Nature*, **387**, 569–570.

Smart,E.J., Mineo,C. and Anderson,R.G.W. (1996) Clustered folate receptors deliver 5-methyltetrahydrofolate to cytoplasm of MA104 cells. *J. Cell Biol.*, **134**, 1169–1177.

Sutterlin,C., Doering,T.L., Schimmoller,F., Schroder,S. and Riezman,H. (1997) Specific requirements for the ER to Golgi transport of GPI-anchored proteins in yeast. *J. Cell Sci.*, **110**, 2703–2714.

Tabas,I., Weiland,D.A. and Tall,A.R. (1985) Unmodified low density lipoprotein causes cholesteryl ester accumulation in J774 macrophages. *Proc. Natl Acad. Sci. USA*, **82**, 416–420.

Taraboulos,A., Serban,D. and Prusiner,S.B. (1990) Scrapie prion proteins accumulate in the cytoplasm of persistently infected cultured cells. *J. Cell Biol.*, **110**, 2117–2132.

Taraboulos,A., Scott,M., Semenov,A., Avraham,D., Laszlo,L. and Prusiner,S.B. (1995) Cholesterol depletion and modification of COOH-terminal targeting sequence of the prion protein inhibit formation of the scrapie isoform. *J. Cell Biol.*, **129**, 121–132.

Tokuyasu,K.T. (1973) A technique for ultracryotomy of cell suspensions and tissues. *J. Cell Biol.*, **57**, 551–565.

Tooze,J. and Hollinshead,M. (1991) Tubular early endosomal networks in AtT20 and other cells. *J. Cell Biol.*, **115**, 635–653.

Trowbridge,I.S., Collawn,J.F. and Hopkins,C.R. (1993) Signal-dependent membrane protein trafficking in the endocytic pathway. *Annu. Rev. Cell Biol.*, **9**, 129–161.

Turek,J.J., Leamon,C.P. and Low,P.S. (1993) Endocytosis of folate–protein conjugates: ultrastructural localization in KB cells. *J. Cell Sci.*, **106**, 423–430.

Varma,R. and Mayor,S. (1998) GPI-anchored proteins are organised in sub-micron sized domains at the cell surface. *Nature*, in press.